2025-32-0047/20259247 Published 03 Nov 2025

Impact of Enhanced Physics-Based Estimation Modeling for Trapped Air and EGR in Real-Time Control of Hydrogen Injection in a PFI Internal Combustion Engine

Claudio Galli, Giovanni Ferrara, Niccolò Grilli, Francesco Balduzzi, and Luca Romani Università degli Studi di Firenze

Giovanni Vichi Yanmar R&D Europe

Citation: Galli, C., Ferrara, G., Grilli, N., Balduzzi, F. et al., "Impact of Enhanced Physics-Based Estimation Modeling for Trapped Air and EGR in Real-Time Control of Hydrogen Injection in a PFI Internal Combustion Engine," SAE Technical Paper 2025-32-0047, 2025, doi:10.4271/2025-32-0047.

Received: 16 May 2025 Revised: 16 Jul 2025 Accepted: 21 Jul 2025

Abstract

Hydrogen PFI engines face abnormal combustion issues, especially during transient operation. The air-to-fuel ratio and trapped exhaust gas significantly affect combustion stability and NOx emissions, requiring continuous monitoring. Real-time estimation of the trapped gas composition and thermodynamic state is therefore crucial but challenging.

This work introduces a real-time, physics-based Multi-Input-Multi-Output (MIMO) model for accurately estimating trapped air and exhaust gas mass at the intake valve closing (IVC) event. In detail, the estimation model makes use of dynamic in-cylinder and exhaust pressure measurements to accurately model mass flows and heat exchange equations with 0.5 CAD resolution. This allows extremely high fidelity when modelling the physical properties of the various chemical species along the engine cycle. Moreover, the model calibration appears only in the form of two coefficients implemented on a lookup table for twelve different operating points, highlighting the small calibration effort.

The physics-based model for the estimation of the amount of air and EGR was validated against 1-D numerical results for a hydrogen-fueled PFI engine prototype developed in GT-Power environment. The validation process analyzes the model accuracy in multiple steady-state and transient profiles, in terms of in-cylinder trapped air and residuals. 165 steady cases and two transient profiles of 1800 engine cycles each are studied. Results show the robustness and accuracy of the model, allowing proper AFR control especially when integrating a fuel-injection correcting controller. Indeed, value of normalized mean absolute percentage error around 2% and 5% are reported for air and EGR estimation. The model proves to be highly accurate even in fast-transient operation: however, further improvements will be carried out to reduce maximum errors observed.

Introduction

In the pursuit of sustainable transportation and energy production, hydrogen-powered internal combustion engines have emerged as a promising alternative due to their potential to significantly reduce greenhouse gas emissions without relying solely on electrification [1]. These engines however face challenges such as abnormal combustion events like backfires or pre-ignitions, hindering widespread usage [2]. Research has established a strong correlation between in-cylinder trapped air charge, trapped burnt gas, and the occurrence of abnormal combustion events [3]. Precise models are therefore necessary to estimate trapped air mass and exhaust gas recirculation (EGR) to enhance the reliability of H_2 internal combustion engines (ICEs) for wider use.

Several solutions have been proposed by various researchers to accurately estimate key parameters such as air charge, air-to-fuel ratio (AFR), and EGR in internal combustion engines. Wang et al. [4] conducted an extensive review of current air mass estimation techniques, focusing particularly on spark ignition (SI) engines. Modelling approaches can be categorized into four main groups: utilization of MAF/MAP sensors, input estimation methods, speed-density approaches, and implementation of closed-loop observers such as Kalman filters, with other methods being less common. Jankovic et al. [5] developed a MATLAB/Simulink model to predict trapped air mass using inputs from a MAP sensor and EGR throttle valve position. The model, calibrated with empirical coefficients, was validated in steady and transient operations

for a gasoline 4L truck engine. In contrast, Kumar et al. [6] applied a discrete model for in-cylinder AFR estimation, incorporating a Kalman filter for feedback control of air-fuel ratio without lambda sensors. The model was experimentally validated on a gasoline engine test bench, demonstrating high accuracy and reduced over/undershoots. Arsie et al. [7] utilized in-cylinder pressure measurements to develop two algorithms based on pressure ratios and moments, capable of estimating in-cylinder AFR, with the pressure ratio algorithm performing particularly well in lean operation regions.

To estimate EGR, Klein et al. [8] developed two empirical models of varying complexity to estimate in-cylinder EGR fraction, primarily using in-cylinder pressure as the main input and calibration coefficients to achieve accurate estimation. Both models were validated in steady and transient operating conditions.

Khameneian et al. [9] proposed a real-time, physics-based model for estimating the air mass and EGR trapped at intake valve closure (IVC). The algorithm uses dynamic pressure measurements from the intake, exhaust, and in-cylinder locations as inputs and relies on two calibration constants. The Multi-Input-Multi-Output (MIMO) model was validated for a gasoline direct injection (GDI) engine under both steady-state and transient conditions. Validation was performed through numerical simulations and experimental tests, demonstrating minimal over- and underestimation of air charge and internal residual gases. Despite the panorama of modelling techniques available in the literature for the estimation of in-cylinder air and EGR mass a physics-based model specifically developed for a hydrogen-fueled port fuel injection (PFI) and aimed at real-time controlling the fuel injection (embedded implementation) was missing. Indeed, the authors of this paper had proposed a first iteration of a model of trapped air and residuals estimation [10]. The model, coupled with a double PI controller, features simplified physical modeling with around 8 dynamic in-cylinder and exhaust pressure measurements along the cycle. While as a first attempt the estimation framework showed good results, its integration in transient events reported too high errors which hindered the fuel controller's performance.

The rationale of this work therefore aims at significantly improving the estimation model via increased physical fidelity and better exploitation of in-cylinder and exhaust dynamic pressure measurements along the cycle. The main goals are improved estimation accuracy, robustness and reduced calibration efforts.

This work focuses on the development of a MATLAB-Simulink model based on thermodynamic principles and one-dimensional flow equations, designed to accurately estimate IVC parameters for a hydrogen PFI engine. The model is specifically designed for real-time control applications and intended for integration into the ECU, ensuring functionality under steady and transient conditions. The primary objective of the embedded model is to enable cycle-by-cycle control of the injected fuel quantity: when the estimated air and EGR masses approach critical thresholds, the fuel injection is reduced to prevent abnormal combustion phenomena. The structure of the study is as follows: the *Multi-Input Multi-Output estimation model* section describes the computational framework, detailing the methodology and rationale behind the developed model equations, with emphasis on key features and assumptions. Then, the *Experimental and numerical MIMO validation* section outlines the specific case study under investigation along with the corresponding experimental setup and numerical validation model. The *Results* section presents the findings, including a thorough sensitivity analysis and comparisons under both steady-state and transient conditions. Finally, the *Conclusions* section summarizes the main takeaways of the study.

Multi-Input Multi-Output Estimation Model

The EGR and air charge physics-based model was developed starting from a previous iteration carried out by the authors in [10]. This first approach made use of simplified modeling and only some in-cylinder and exhaust pressure measurements along the cycle. Moreover, model calibration was a slow process which required fine tuning of two parameters. In the current paper, the authors aim at improving physical modeling and better exploit the use of the expensive dynamic in-cylinder and exhaust pressure sensor. The goal was to improve accuracy for trapped air and residuals estimation and reduced calibration efforts.

The trapped air mass and residual EGR estimation model was developed in MATLAB Simulink using a modular and physics-based approach. Each simulation cycle runs from Exhaust Valve Opening (EVO) to Intake Valve Closing (IVC), with in-cylinder temperature estimated throughout to improve accuracy in air and EGR mass calculations. The model's primary input is high-resolution (0.5° CA) dynamic pressure data from the cylinder and exhaust. Additional inputs include average intake pressure and temperatures of the intake air, fuel, and coolant.

Two key calibration parameters, for in-cylinder temperature correction at EVO and a convective heat transfer coefficient for the intake phase, were tuned using data from twelve operating points. These were then implemented as lookup tables based on engine speed and load (IMEP) to ensure accurate trapped air and EGR estimation across conditions.

The model runs once per cycle at IVC, calculating the trapped air mass to enable precise fuel injection control with a delay of one engine cycle (due to PFI injection approaches). Figure 1 provides an overview of the model, emphasizing its input and output in sequential modeling for estimating a single cycle.

In the equations presented below, as illustrated in Figure 1, the index [k] denotes the current engine cycle, beginning at exhaust valve opening (EVO) and ending at intake valve closing (IVC). The indices [k–1 and [k+1] correspond to the previous and subsequent engine cycles, respectively.

FIGURE 1 Representation of the Simulink estimation model.

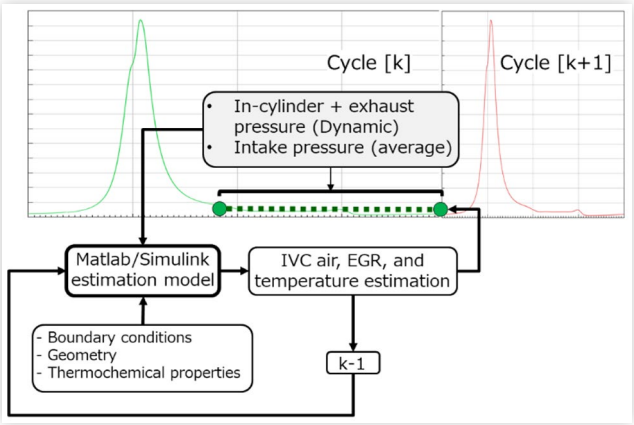

The next section provides a detailed description of the model's equations and overall structure.

Detailed Model Description

The model iteration starts at EVO and end at IVC. The estimation model is modular, meaning that it divides the engine in six segments applying different physics equation to accurately estimate temperatures and trapped masses where needed.

IVC to EVO

In the first segment of the cycle, the combustion process is not modelled. Instead, using trapped air, fuel and residuals from previous cycles EVO temperature (T_{EVO}) is obtained using the ideal gas law as in Equation 1. IVC and EVO are set at CAD of -128° and +138° respectively, being the reference 0° at firing top dead centre.

$$T_{EVO}[k] = \frac{x \cdot P_{EVO}[k] \cdot V_{EVO}}{\left(m_{AIR}[k-1] + m_{FUEL}[k-1] + m_{EGR}[k-1]\right) \cdot R_{EXH}} \quad (1)$$

Where:

- P_{EVO} is the in-cylinder measured pressure at EVO [Pa]
- V_{EVO} is the in-cylinder volume at EVO [m^3]
- m_{AIR}, m_{FUEL}, m_{EGR} are respectively the in-cylinder trapped air, fuel and residual gases. These values are obtained at previous cycle Intake Valve Closing position, hence why the [k-1] index.
- R_{EXH} is the specific gas constant of exhaust gases, calculated in function of the assumed operating AFR and equal to 313.85 J/(K*kg)
- x is the first calibration factor of the model, and it is tweaked to match the EVC trapped mass m_{EVC}. It represents a correction factor at the start of the estimation model that removes initial error bias which may be present due to the various assumptions along the cycle.

EVO to BWD

The following formulation is carried out from EVO to end of blowdown (BWD) using the isentropic flow equation to obtain the end of blowdown temperature (T_{BWD}), as shown in Equation 2.

From now on, in the following equations reported in this paper, the subscript θ will be used to indicate 0.5 CAD formulations: therefore, θ is the CAD index of the quantity observed at the current crank angle degree while θ-1 indicates the previous CAD. In particular, the end of blowdown point is assumed when exhaust and in-cylinder pressure are equal and therefore is different for each cycle: if this does not happen, the point where the two pressures are closer is used.

Hence, Equation 2 is run from the EVC angle of +138° up to the BWD variable angle.

$$T_{BWD,\theta}[k] = T_{BWD,\theta-1}[k] \cdot \left(\frac{P_{BWD,\theta}[k]}{P_{BWD,\theta-1}[k]} \right)^{\frac{\gamma_{EXH}-1}{\gamma_{EXH}}} \quad (2)$$

Where:

- P_{BWD} is the in-cylinder measured pressure at end of Blowdown [Pa]
- γ_{EXH} is the Cp/Cv ratio observed during the exhaust phase, obtained from GT-Power simulations and imposed equal to 1.3316

Once the temperature at BWD is obtained by iterating Equation 2 until the BWD crank angle is reached, the in-cylinder trapped mass at end of blowdown can be obtained via the ideal gas law equation (Equation 3):

$$m_{BWD}[k] = \frac{P_{BWD}[k] \cdot V_{BWD}[k]}{R_{EXH} \cdot T_{BWD}[k]} \quad (3)$$

With V_{BWD} being the in-cylinder volume at end of blowdown [m^3]. Differently from other volumes used in the various equation, this value changes depending on in-cylinder and exhaust pressure during the exhaust phase, hence why the [k] index is applied.

BWD to IVO

From end of blowdown to Intake Valve Opening (IVO), the energy balance equation is applied to estimate the IVO temperature (T_{IVO}) during the exhaust phase for every angle step. The IVO angle is fixed and set at +338°. Therefore, Equation 4 to Equation 9 are applied from the previously set BWD angle up to +338°.

$$-Q_{IVO,\theta}[k] + W_{IVO,\theta}[k] - H_{IVO,\theta}[k] = \Delta U_{IVO,\theta}[k] \quad (4)$$

With Q_{IVO}, W_{IVO}, H_{IVO}, ΔU_{IVO} being respectively the contributions of heat, work, enthalpy and internal energy change during the exhaust phase going from BWD to IVO.

The heat contribution Q_{IVO} is formulated via convective heat exchange using Equation 5:

$$Q_{IVO,\theta}\left[k\right] = h_{EXH}\left[k\right]\cdot A_{CYL,\theta}\cdot\left(T_{CYL,\theta}\left[k\right] - T_{COOLANT}\right)\cdot \frac{\Delta\theta_{EXH}}{6N\left[k\right]} \quad (5)$$

Where:

- A_{CYL_INT} is the in-cylinder area at the current angle [m^2]
- $\Delta\theta_{EXH}$ is the duration in CAD of the current angle step [°]
- $T_{COOLANT}$ is the cylinder coolant temperature, assumed as equal to 350 K
- T_{CYL} is the average in-cylinder intake phase temperature, computed as mean value between current in-cylinder temperature ($T_{IVO,\theta}$ the equation unknown) and exhaust manifold measured temperature [K]
- h_{EXH} is the convective heat exchange coefficient of the exhaust phase. This value is obtained from GT-Suite steady simulations and imposed equal to 35 W/(K*m^2)

Differently, the work contribution W_{IVO} can be computed as shown in Equation 6:

$$W_{IVO}\left[k\right] = P_{IVO,\theta}\left[k\right]\cdot\Delta V_{IVO,\theta} \quad (6)$$

With $\Delta V_{IVO,\theta}$ being the volume difference at every angle step during the exhaust phase [m^3]. The enthalpy contribute H_{IVO} is similarly formulated using Equation 7:

$$H_{IVO}\left[k\right] = P_{U,\theta}\left[k\right]\cdot\Delta V_{IVO,\theta} \quad (7)$$

With P_U indicating the upstream pressure between the in-cylinder and exhaust measured pressure [Pa]. Instead, the contribution of internal energy change ΔU can be computed as of Equation 8:

$$\Delta U_{IVO}\left[k\right] = m_{IVO}\left[k\right] * C_{v_{EXH}} * \left(T_{IVO,\theta}\left[k\right] - T_{IVO,\theta-1}\left[k\right]\right) \quad (8)$$

To obtain the trapped in-cylinder mass m_{IVO} for every 0.5 CAD the exhaust valve mass flow m_{IVO} is computed using the isentropic flow equation as of Equation 9:

$$\dot{m}_{IVO,\theta}\left[k\right] = \pm\frac{n_{VLV} * A_{EFE,\theta} * P_{U,\theta}\left[k\right]}{\sqrt{T_U\left[k\right] * R_{EXH}}}\cdot\left(\frac{P_{D,\theta}\left[k\right]}{P_{U,\theta}\left[k\right]}\right)^{\frac{1}{\gamma_{EXH}}}\cdot \left\{\frac{2\cdot\gamma_{EXH}}{\gamma_{EXH}-1}\cdot\left[1-\left(\frac{P_{D,\theta}\left[k\right]}{P_{U,\theta}\left[k\right]}\right)^{\frac{\gamma_{EXH}-1}{\gamma_{EXH}}}\right]\right\}^{\frac{1}{2}} \quad (9)$$

Where:

- n_{VLV} is the number of exhaust valves
- T_U and P_D are respectively the upstream temperature [K] and downstream pressure [Pa] depending on the in-cylinder and exhaust measured pressures
- A_{EFF} is the effective exhaust valve area measured at the test bench and mapped for every half CAD [m^2]

Total trapped mass at IVO m_{IVO} can be obtained simply following Equation 10:

$$m_{IVO}\left[k\right] = m_{BWD}\left[k\right] + \sum_{\theta=BWD}^{\theta=IVO}\Sigma\dot{m}_{IVO,\theta}\left[k\right] \quad (10)$$

This allows us to obtain every needed quantity to apply Equation 4 from BWD angle to IVO and obtain IVO temperature T_{IVO} and in-cylinder trapped mass m_{IVO}. In particular, the equation system which combines Equations 4 to 9 can be solved in the form of a second-degree equation in function of T_{IVO},

IVO to EVC

After the exhaust phase, the in-cylinder goes through a positive valve overlap: both the exhaust and intake valves are open and in-cylinder EVC temperature T_{EVC} can be obtained from the isentropic expansion equation (Equation 11). Being the EVC angle fixed and set at -338°, Equation 11 and Equation 12 are used from +338° to -338°.

$$T_{EVC,\theta}\left[k\right] = T_{EVC,\theta-1}\left[k\right] * \left(\frac{P_{EVC,\theta}\left[k\right]}{P_{EVC,\theta-1}\left[k\right]}\right)^{\frac{\gamma_{OV}-1}{\gamma_{OV}}} \quad (11)$$

Indeed, isentropic mass flow equation can be again used to model the exhaust valve flow $\dot{m}_{OV}$ inside or outside the cylinder depending on the pressures as of Equation 12.

$$\dot{m}_{OV,\theta}\left[k\right] = \pm\frac{n_{VLV} * A_{EFF,\theta} * P_{U,\theta}\left[k\right]}{\sqrt{T_U\left[k\right] * R_{EXH}}}\cdot\left(\frac{P_{D,\theta}\left[k\right]}{P_{U,\theta}\left[k\right]}\right)^{\frac{1}{\gamma_{OV}}}\cdot \left\{\frac{2\cdot\gamma_{OV}}{\gamma_{OV}-1}\cdot\left[1-\left(\frac{P_{D,\theta}\left[k\right]}{P_{U,\theta}\left[k\right]}\right)^{\frac{\gamma_{OV}-1}{\gamma_{OV}}}\right]\right\}^{\frac{1}{2}} \quad (12)$$

With γ_{OV} being the Cp/Cv ratio observed during the overlap phase, obtained from GT-Power steady simulations and imposed equal to 1.3384. Then, in-cylinder trapped mass at EVC m_{EVC} can be simply computed by adding the integrated mass flow throughout the overlap period as shown in Equation 13.

$$m_{EVC}\left[k\right] = m_{IVO}\left[k\right] + \sum_{\theta=IVO}^{\theta=EVC}\Sigma\dot{m}_{OV,\theta}\left[k\right] \quad (13)$$

EVC to cBDC

In the intake section, a 0.5 CAD calculation like the ones observed before cannot be used. This is due to the fact that the composition of the intake fluid mixture cannot be known with such high resolution. Indeed, in PFI engines, air and fuel both flow inside the cylinder during the intake phase, often in a non-homogenous way along the intake phase as well. Moreover, while not specific for this case study, an additional problem in fine 0.5 CAD modeling would also be relevant to the presence of external EGR, which would introduce another unknown in the problem. Therefore, exclusively to this section of the cycle, a segmented modeling is used equal to the one presented in [10]. The introduction of another calibration coefficient h_{INT}, in the form of the convective heat exchange coefficient is needed. This allows us to obtain the in-cylinder temperature at IVC T_{IVC}, together with the trapped moles and mass of fuel, air and residuals.

cBDC to IVC

In the last step, the polytropic compression equation is used to obtain the IVC temperature T_{IVC} (Equation 13) from the piston compression Bottom Dead Center angle (cBDC) at -180° as of Equation 14. This modeling approach is used from -180° up to the IVC angle at -128°.

$$T_{IVC,\theta}[k] = T_{IVC,\theta-1}[k]\cdot\left(\frac{P_{IVC,\theta}[k]}{P_{IVC,\theta-1}[k]}\right)^{\frac{n_p-1}{n_p}} \quad (14)$$

With n_p being the compression polytropic index, obtained from GT-Power steady-state simulations and imposed equal to 1.55. With know temperature, IVC total trapped moles n_{IVC} can be obtained with IVC pressure, temperature, and volume by applying the Ideal Gas Law as in Equation 15.

$$n_{IVC}[k] = \frac{P_{IVC}[k]\cdot V_{IVC}}{R_U\cdot T_{IVC}[k]} \quad (15)$$

Where:

- n_{IVC} are total trapped moles at IVC [mol]
- V_{IVC} is the in-cylinder volume at IVC [m^3]

Then, IVC trapped air mass m_{AIR} is calculated as the newly obtained n_{IVC} and subtracting the trapped moles of fuel and residuals (Equation 16). Intake backflow of exhaust gases and fuel during the piston rise is ignored as said backflow is expected to enter in-cylinder in the following cycle intake phase.

$$m_{AIR}[k] = \left(n_{IVC}[k] - \frac{m_{FUEL}[k-1]}{M_{FUEL}} - \frac{m_{EGR}[k]}{M_{EGR}}\right)\cdot M_{AIR} \quad (16)$$

FIGURE 2 Simple scheme of the MIMO modeling structure along the cycle

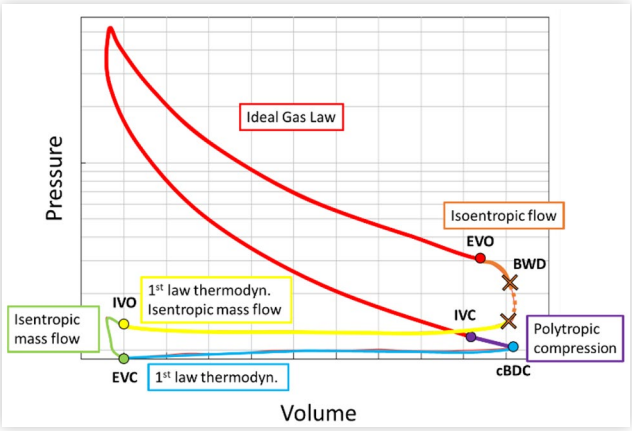

Where:

- m_{FUEL} is the quantity of injected fuel at the previous cycle [kg]
- M_{FUEL}, M_{EGR} and M_{AIR} are the molecular weight of the fuel, residuals and air equal to 2.016, 28.96 and 26.49 g/mol respectively
- m_{EGR} is the quantity total trapped residuals [kg]. It assumed that trapped EGR at IVC are equal to m_{EVC}: meaning that no residuals backflow is observed during the intake phase.

This last step estimates in-cylinder trapped air at IVC. The injection process then happens by simply dividing the IVC estimated trapped air with the target AFR. This allows proper fuel injection control with as little as one cycle of delay, as at IVC the injection has already stopped, and combustion is starting.

This step concludes the temperature and mass modeling inside the cylinder. The iteration procedure is then carried out for the following cycle by starting again from Equation 1.

In summary, the modeling structure can be clearly visualized in Figure 2, where the different segments of the cycles and notable θ events are highlighte in a P-V diagram (Pressure in logarithmic scale). Moreover, the angle of end of Blowdown (BWD) is reported in dashed line to show its variable range, differently from all other.

Engine Case Study

Experimental Setup

Developing a numerical estimation embedded model for real-time control of hydrogen-fueled engines involves both experimental and simulation-based steps, as incorrect fuel injections can cause severe engine damage. In this work, a transient GT-Suite model was created to accurately simulate the behavior of a hydrogen engine

and operate in a model-in-the-loop (MIL) setup with the MIMO controller. This setup enabled calibration and validation of the MIMO model's real-time performance. The GT-Suite model was based on a YANMAR four-stroke heavy-duty engine, thoroughly tested at the hydrogen facility of the L.In.E.A. Laboratory, University of Florence.

The hydrogen-fueled engine studied is a 2.2-liter, four-cylinder prototype derived from the commercial YANMAR 4TN88G natural gas engine. For testing, it was operated in single-cylinder mode, with the other three cylinders motored in a closed-valve configuration and external EGR duct closed off.

The hydrogen test facility at the L.In.E.A. Laboratory includes an 80-kW motored engine test bench (1000–3000 rpm), a 74-kW commercial electrolyzer, and a mechanical pressure regulation system. Hydrogen is treated before engine injections via a dryer which uses salts to curb water content. Both steady-state and dynamic measurements are performed to evaluate combustion and engine performance. Key instrumentation includes sensors for hydrogen flow, air-fuel ratio, temperatures, emissions, and in-cylinder pressure. Data acquisition and analysis are handled through custom CoBa software and AVL systems, with high-resolution sampling and knock analysis capabilities. Full setup details are available in references [10, 11]. A scheme of the experimental measurement layout is presented in Figure 3.

The engine prototype was meticulously calibrated in this study to ensure stable combustion under fuel-lean conditions. A balanced compromise between engine performance, thermal-mechanical stress, and NOx emissions was achieved at λ = 2 across nearly the entire operating range. Spark timing was adjusted to the most fuel-efficient point while preventing knock, and the Start of Injection (SOI) was fixed at 360°CA before firing Top Dead Center (TDC).

FIGURE 3 Measurement system layout [10].

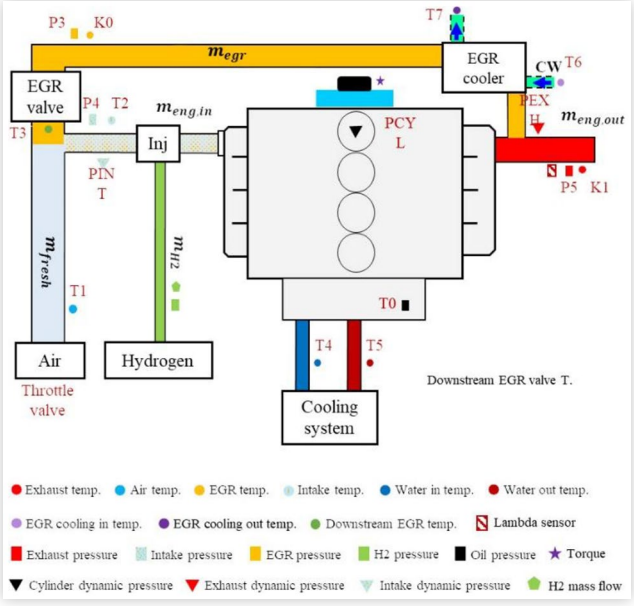

GT-Suite Engine Model

The MIMO model developed in this study is tailored towards for real-time applications, with the goal of accurately estimating the fresh air and EGR (exhaust gas recirculation) levels in the engine cylinder to enable precise fuel injection control. Its development involves two preliminary GT-Suite models: one steady-state model using the Three Pressure Analysis (TPA) for calibrating air and EGR estimates, and another transient model using the Wiebe function to simulate dynamic engine behavior. The study focused solely on the in-head injector and used experimental calibration data limited to λ=2 conditions. Additional details on the modeling methods are provided in reference [12]. The steady-state TPA model includes the engine, cylinder head ducts, intake and exhaust systems, throttle valve downstream intake duct, and the PFI injector. It uses 100-cycle averaged dynamic pressure profiles and steady-state temperatures as boundary conditions, including in-cylinder pressure profiles. Heat exchange is modeled via finite element analysis using coolant and oil temperatures. Simulations cover nine operating points: three engine speeds (1000, 2000, 3000 rpm) and three IMEP targets (1.2, 3.6, 5.5 bar) at constant λ of 2. The model outputs include volumetric and trapping efficiency, fuel quantity, internal EGR, and in-cylinder pressure profiles generated via the Wiebe function.

The transient model builds upon the TPA model, extending it to include the full intake and exhaust systems, including the throttle body and muffler. Ambient pressure and temperature are applied at the boundaries. It reuses the TPA heat exchange model and applies trilinear interpolation of TPA data to map combustion parameters (Wiebe exponent, MFB duration and position) and fuel quantities. Injection mapping is refined to meet target IMEP levels under varying loads. A PID-controlled steady-state model generates a 35-point throttle position map for λ of 2, used in the transient model. As an example, Figure 4 shows the pressure trend at 3000 rpm and 3.6 bar IMEP provided by the TPA model (compared to the

FIGURE 4 P-V diagram at 3000 rpm and 3.6 bar IMEP [10].

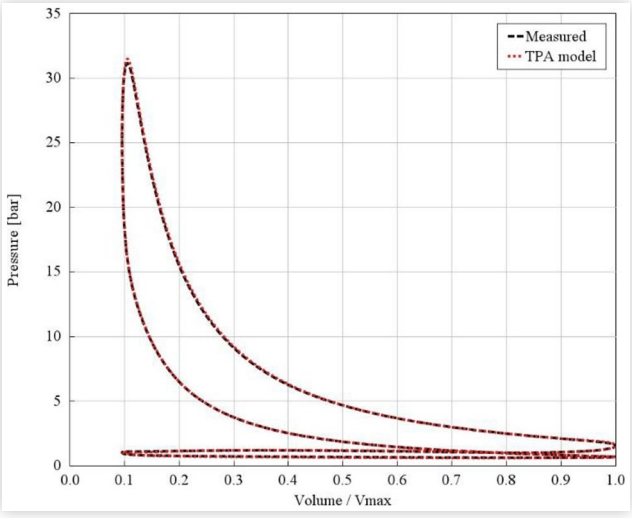

experimental measurement). Considering all the nine investigated points, an average (maximum) RMSE of 2.61% (6.05%) was observed in terms of IMEP and 2.85% (5.32%) in terms of maximum pressure.

While combustion and throttle maps are embedded in GT-Suite, the injection map is handled in Simulink, integrated via a Simulink harness. With these calibrated maps, the transient model accurately simulates engine behavior across a range of 1–5.5 bar IMEP and 1000–3000 rpm, effectively covering real operating conditions. More details are provided in [10].

Results

In order to evaluate the reliability and effectiveness of the developed MIMO model, the estimated values of internal EGR and in-cylinder trapped air mass were analyzed in both steady-state operating points and transient profiles. In detail, the results of the GT-Suite TPA model and the GT-Suite transient model were used to validate the MIMO model in steady-state and transient conditions respectively.

The model was celebrated at 12 steady points, for:

- 3 values of speed (1000, 2000 and 3000 RPM)
- 4 values of load (1.4, 2.4, 3.6 and 5.5 bar IMEP)

This allows the development of 2D lookup table for the model calibration coefficients x and h_{INT}. Once the coefficients are calibrated and implemented on said lookup table in function of speed and load, the model is ready to be used for temperature and trapped mass estimation.

Moreover, a detailed statistical analysis of the estimation error for both steady and transient operation is carried out. To evaluate the accuracy of the prediction model, the following error metrics are introduced:

- *Normalized Root Mean Square Percentage Error (NRMSPE)*: the main parameter for prediction error evaluation. Indeed, RMSPE is the target of the minimization process carried out in the optimization process. RMSPE is often regarded as the most important error evaluation parameter because of its sensitivity to bigger errors or outliers [13]. NRMSPE computation is reported in Equation 16:

$$NRMSPE = \frac{100}{y_{AVG}} \cdot \sqrt{\frac{1}{n}\sum_{i=1}^{n}\left(y_i - p_i\right)^2} \tag{16}$$

Where:

- n is the number of predicted values, in this case the number of analyzed engine cycles
- y_i is the current value of trapped air or residuals [mg]
- y_{AVG} is the average value of trapped air or residuals [mg]
- p_i is the estimated value of trapped air or residuals [mg]

- *Normalized Mean Absolute Percentage Error (NMAPE)*: calculated as in Equation 17, this metric reports the average differences between each pair of estimated and actual values. Therefore, compared to RMSPE, each error is treated independently from its size. This value therefore provides a clear indicator of the general error observed.

$$NMAPE = \frac{100}{y_{AVG} \cdot n}\sum_{i=1}^{n}\left|y_i - p_i\right| \tag{17}$$

- *Maximum overshoot (err_{MAX+}) and maximum undershoot (err_{MAX-})*: the maximum error produced, both positive (Equation 18) and negative (Equation 19) by the estimation model. This value results of crucial importance. Depending on the application, a model with higher RMSE or MAE could be preferred over
a more accurate one if maximum errors are lower.

$$err_{MAX+} = 100 \cdot MAX\left(\left(y_i - p_i\right) / y_i\right) \tag{18}$$

$$err_{MAX-} = 100 \cdot MIN\left(\left(y_i - p_i\right) / y_i\right) \tag{19}$$

Steady State Validation

The capability of the MIMO model of estimating the air and EGR amount inside cylinder was first tested in multiple steady-state operating points to address the model accuracy in a scenario free of errors due to delay or transient events. Indeed, a total of 165 steady state cases are analyzed: the specific values of speed and load of each simulation are reported in Table 1.

The comparison between results from the MIMO and GT-Suite TPA models focused on IVC trapped air mass and trapped EGR mass, as illustrated in Figure 5 scatter plot. In this figure, the black line denotes a direct correspondence between the values predicted by the MIMO model and those simulated by the GT-Suite, while red lines indicate 10% error confidence bands. The X-axis label is labeled as “Measured” in this context since experimental data is typically unavailable for such values, particularly trapped EGR. Indeed, while quantities of trapped air can be precisely estimated, residuals fraction measurements are more complex: therefore, GT-Suite model values are used as reference.

As can be observed from trapped air scatter plot in Figure 5(a), the estimation is often within the 10% error band: only 2 instances of the 165 analyzed ones are outside the error band and both represent

TABLE 1 steady operation simulated scenarios

Variable	MIN	MAX	Resolution	n. cases
Speed [RPM]	1000	3000	200	11
IMEP [bar]	1.4	5.5	0.3	15

FIGURE 5 Steady state estimation accuracy of trapped air a) and residuals b).

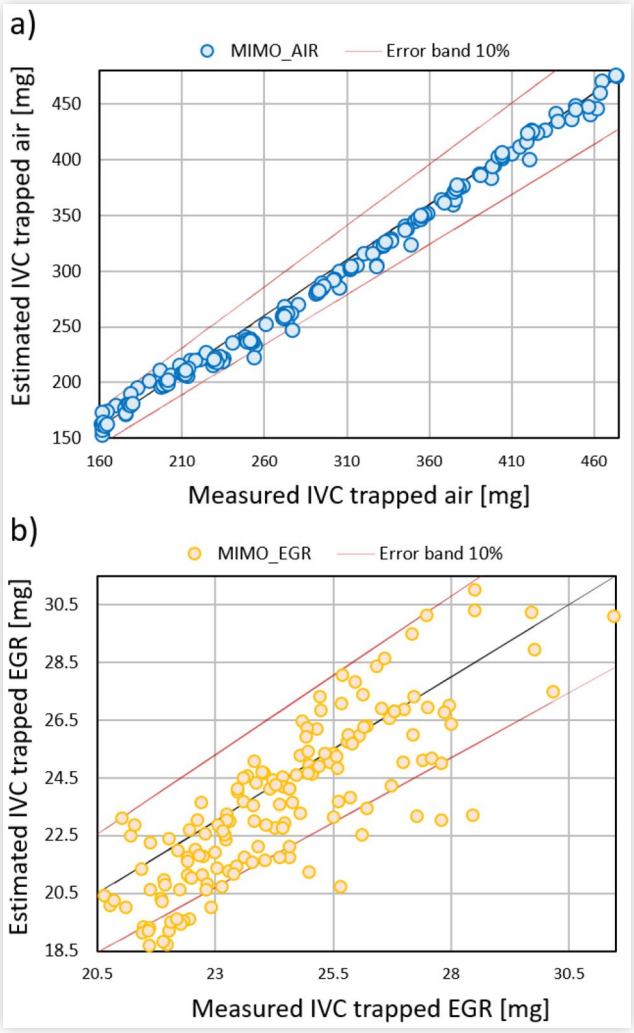

FIGURE 6 profiles of speed and imposed load for the two transient profiles.

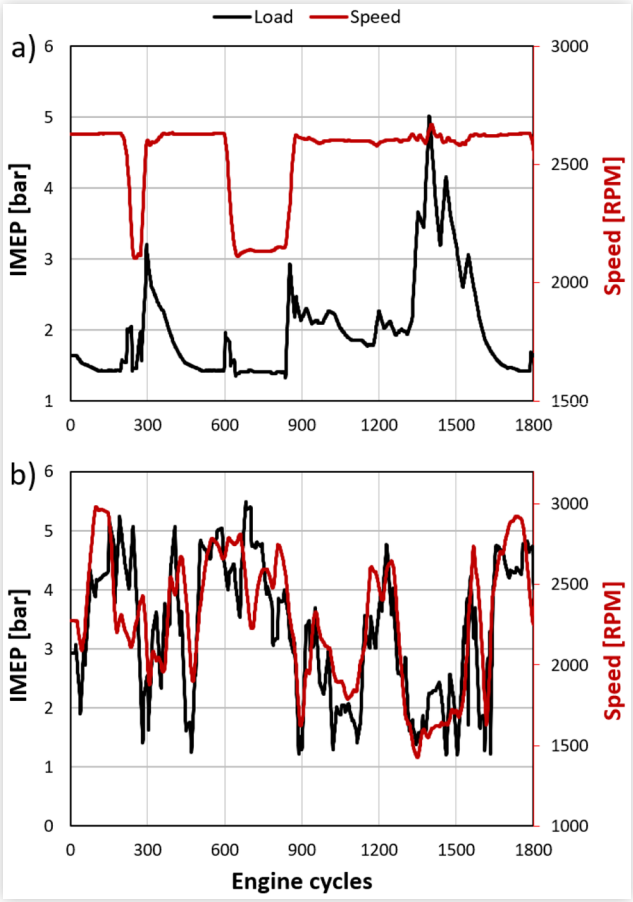

underestimations compared to the actual values in low-load zone operation. In general, the model appears to overestimate for extremely low values of trapped air at IVC while instead a general underestimation is shown.

Differently, Figure 5(b) reports the scatter plot for trapped residuals. This time, 20 critical instances are shown, and all appear as underestimation errors as well. Moreover, the overall accuracy of the estimation model is lower than the one observed for trapped air. Indeed, a higher error is more probable for residuals, as the mass is about one order of magnitude smaller than air.

Transient Validation

Despite the satisfying results of the steady-state validation, which highlight the model robustness, the goal of use of the developed MIMO model requires a detailed reliability investigation during load and speed variations. Two transient profiles of 1800 engine cycles have been studied. The first studied profile (Figure 6(a)) includes mild load and speed variations, moreover, a general situation of low load and high speed is observed. Differently, the second transient reported in Figure 6(b) provides more challenging speed and load variations, ranging quickly across the whole engine operating range. To improve readability, from now on we will refer to "Profile A" and "Profile B" for the transient cycles observed in Figure 6(a) and Figure 6(b) respectively.

The developed numerical model is then applied in open-loop simulation to compare the estimated trapped air and residuals with the real GT-Suite model. In detail, Figure 7 shows a direct comparison in terms of trapped air at IVC with Figure 7(a) referring to Profile A and Figure 7(b) for Profile B. An error band of ±10% is introduced to better visualize the model estimation accuracy. As it can observed, trapped air estimation never exceeds such limit for Profile B but some critical events (around engine cycles number 1500) are shown for Profile B instead. Generally, however, very good accuracy for trapped air estimation is shown for both transient profiles.

A similar comparison analysis is carried out in Figure 8 as well, where the estimated mass of trapped residuals is confronted with the GT-Suite value once again for Profile A and Profile B in Figure 8(a) and Figure 8(b) respectively. This time, in Profile A some significant errors above 10% are shown in the situation of extremely low load (engine cycles 250-300, 500-600 and 1700-1750), but high

FIGURE 7 trapped air estimation for Profile A and Profile B.

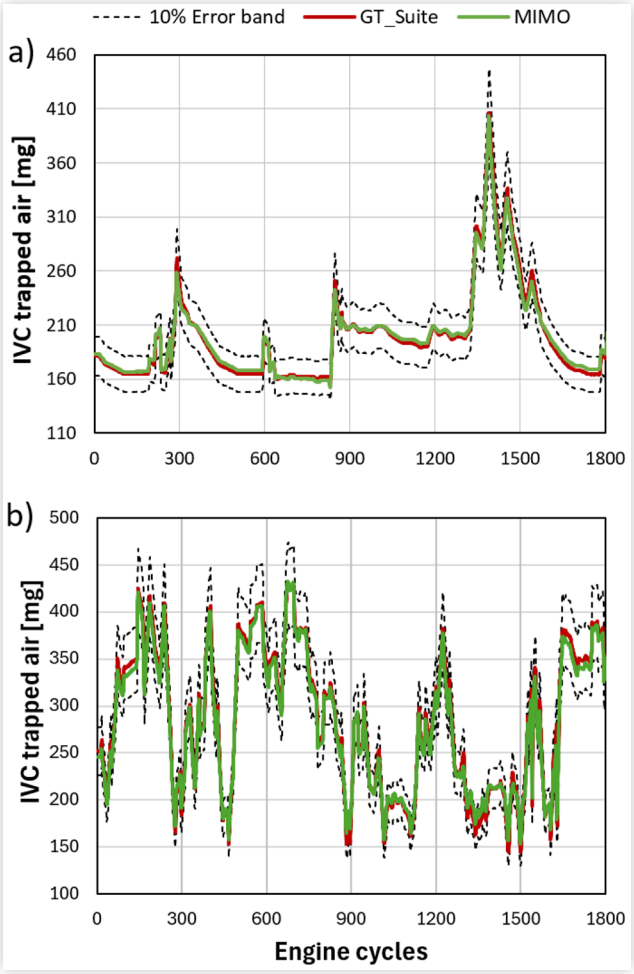

FIGURE 8 trapped EGR estimation for the two analyzed transient profiles.

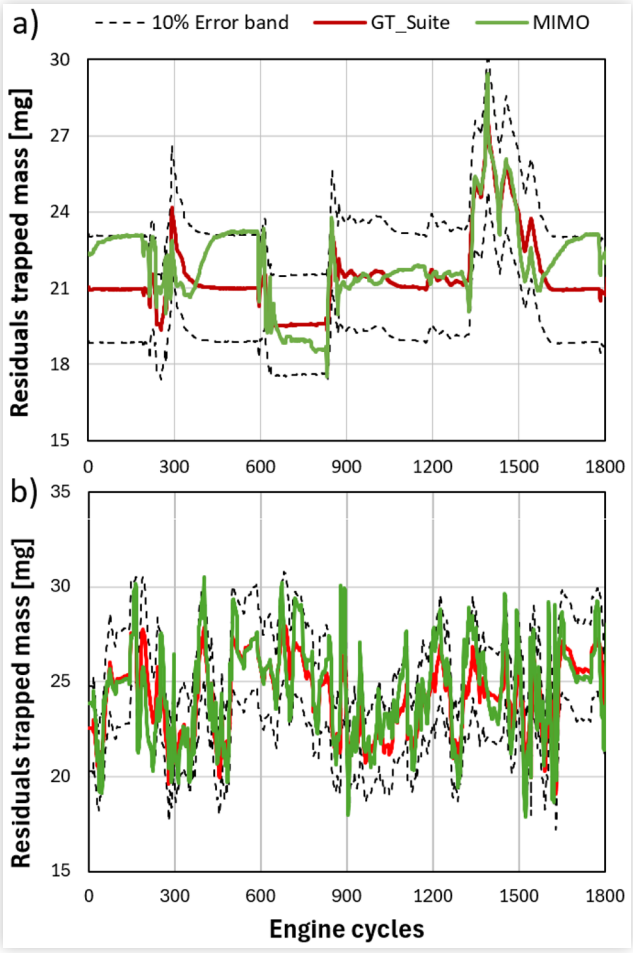

accuracy is observed at higher-load operation. In Figure 8(b) fast speed and load oscillations generate an overall lower accuracy, but the model still provides estimation generally within the ±10% error. Fast load downward transient events at low speeds are however Problematic as they lead to significant oscillations that can observed around engine cycle 900 and 1600.

Indeed, results shown in Figure 7 and Figure 8 can be summarized more clearly in Figure 9, which report the trapped air and residuals percentage error for both Profile A in Figure 9(a) and Profile B in Figure 9(b). Previous model criticalities are better highlighted: for Profile A, the good accuracy of trapped air can be observed together with the higher errors for residuals estimation at low loads.

Statistical Error Analysis

The previously reported figures graphically highlight the model estimation accuracy for the 165 steady cases and the two transient profiles of 1800 engine cycles in terms of trapped air and trapped residuals at IVC.

In Table 2 and Table 3, trapped air and residuals errors are respectively reported for the analyzed steady and transient simulations to more clearly report the estimation model accuracy. Looking at Table 2, it can be observed that trapped air average accuracy is extremely high no matter what the application or the metric used. Indeed, some critical errors are observed especially for transient Profile B, which reports both under and overestimation maximum error above the critical threshold of 10%. While the milder transient does not report critical issues, steady application a maximum error of 12.34% is reported.

Instead, when evaluating EGR estimation, a worse accuracy is overall observed. This can be seen for both NRMSPE and NMAPE in steady and transient application, which shows an increase of around 4-5% when compared to the air counterpart. Moreover, critical estimation errors are also now higher in value and more common, as they appear in both transient profiles and steady application.

Indeed, the model shows good accuracy results and significant improvements over the previous iteration which made use of a simpler physics-based modeling approach.

For comparison, results obtained in Profile A using the numerical modeling of [10] following the simplified structure developed in [9] are reported in Table 4. When it comes to residuals estimation, marginal improvements

FIGURE 9 trapped EGR and air percentage error for Profile A and B.

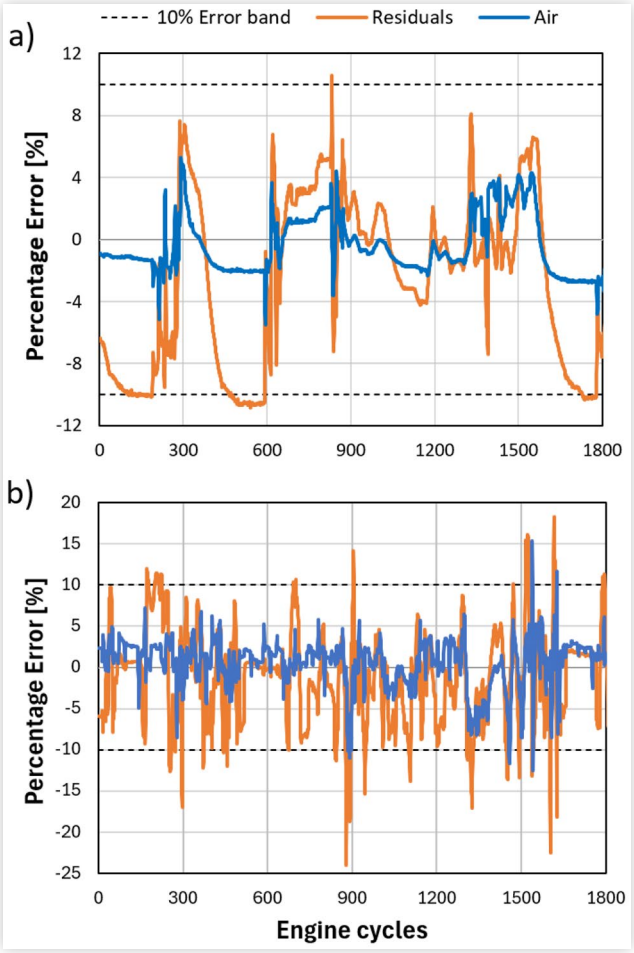

TABLE 2 MIMO trapped air estimation accuracy metrics and errors.

Analyzed scenario	NRMSPE	NMAPE	err_{MAX+}	err_{MAX-}
Steady	3.20%	2.52%	12.34%	-7.05%
Profile A	2.19%	1.67%	5.27%	-5.49%
Profile B	2.60%	2.25%	15.40%	-12.41%

TABLE 3 MIMO trapped EGR estimation accuracy metrics and errors.

Analyzed scenario	NRMSPE	NMAPE	err_{MAX+}	err_{MAX-}
Steady	7.33%	5.74%	19.18%	-9.9%
Profile A	5.95%	4.96%	10.59%	-10.84%
Profile B	5.74%	4.41%	18.31%	-24.07%

are obtained for all the accuracy metrics: yet, the most significant improvements come for trapped air estimation, where accuracy metrics show all errors to be substantially reduced.

However, some criticalities are still observed especially when it comes to trapped residuals' estimation.

TABLE 4 Simplified approach MIMO air and EGR errors (Profile A)

Analyzed quantity (Profile A)	NRMSPE	NMAPE	err_{MAX+}	err_{MAX-}
Trapped air	8.12%	7.90%	18.22%	-17.34%
Trapped EGR	6.28%	5.97%	11.74%	-11.99%

While these errors could be significantly reduced by increasing the calibration points even marginally, the future steps of model development will focus on improved fidelity and physics-based modeling equations.

Conclusions

This work presents a real-time, physics-based Multi-Input Multi-Output (MIMO) model developed to accurately estimate the masses of trapped air and exhaust gas at the intake valve closing (IVC) event. The model leverages dynamic measurements of in-cylinder and exhaust pressures to resolve mass flow and heat exchange processes with a high resolution of 0.5 crank angle degrees (CAD).

A key strength of the approach lies in its minimal calibration requirements: only two coefficients are needed, stored in 2D lookup tables calibrated across twelve operating points. This underscores the model's efficiency and ease of integration for real-world applications. The proposed model was validated using a hydrogen-fueled port fuel injection (PFI) engine prototype simulated in the GT-Power environment. Validation was performed against 1-D numerical results under both steady-state and transient conditions. Specifically, 165 steady operating points and two transient profiles were analyzed to assess estimation accuracy of in-cylinder trapped air and exhaust residuals.

Results demonstrate strong model robustness and precision, particularly in supporting air-fuel ratio (AFR) control when combined with a fuel-injection correction strategy. Normalized mean absolute percentage errors were reported at approximately 2% for air mass and 5% for EGR, with NRMSPE values being slightly higher at around 3% and 6%. However, critical scenarios with absolute percentage errors above 10% are sometimes reported, most frequently for residuals estimation. Indeed, trapped air estimation was shown to be more accurate and robust than residuals estimation no matter the scenario analysed. While the current model performs with high average accuracy, further refinements are planned to reduce peak errors observed.

References

1. Dimitriou, P. and Tsujimura, T., "A Review of Hydrogen as a Compression Ignition Engine Fuel," *Int. J. Hydrog. Energy* 42, no. 38 (2017): 24470-24486, doi:10.1016/j.ijhydene.2017.07.232.

2. Verhelst, S., "Recent Progress in the use of Hydrogen as a Fuel for Internal Combustion Engines," *Int. J. Hydrog. Energy* 39, no. 2 (2014): 1071-1085, doi:10.1016/j.ijhydene.2013.10.102.
3. Szwaja, S., "Dilution of Fresh Charge for Reducing Combustion Knock in the Internal Combustion Engine Fueled with Hydrogen Rich Gases," *Int. J. Hydrog. Energy* 44, no. 34 (2019): 19017-19025, doi:10.1016/j.ijhydene.2018.10.134.
4. Wang, Z., Zhu, Q., and Prucka, R., "A Review of Spark-Ignition Engine Air Charge Estimation Methods," SAE Technical Paper 2016-01–0620 (2016), doi:10.4271/2016-01-0620.
5. Jankovic, M. and Magner, S.W., "Air-Charge Estimation and Prediction in Spark Ignition Internal Combustion Engines," *Proceedings of the 1999 American Control Conference (Cat. No. 99CH36251)* 1: 217, 1999-221, doi:10.1109/ACC.1999.782772.
6. Kumar, M. and Shen, T., "Estimation and Feedback Control of Air-Fuel Ratio for Gasoline Engines," *Control Theory Technol.* 13, no. 2 (2015): 151-159, doi:10.1007/s11768-015-4148-9.
7. Arsie, I., Leo, R.D., Pianese, C., and De Cesare, M., "Estimation of In-Cylinder Mass and AFR by Cylinder Pressure Measurement in Automotive Diesel Engines," *IFAC Proc.* 47, no. 3 (2014): 11836-11841, doi:10.3182/20140824-6-ZA-1003.01602.
8. Klein, P., Grüter, R., and Loffeld, O., "Real-Time Estimation of the Exhaust Gas Recirculation Ratio Based on Cylinder Pressure Signals," SAE Technical Paper 2007-01–0493, SAE International, Warrendale, PA, 2007, doi:10.4271/2007-01-0493.
9. Khameneian, A., Wang, X., Dice, P., Naber, J.D. et al., "A Real-Time Control-Oriented Discrete Nonlinear Model Development for In-Cylinder Air Charge, Residual Gas and Temperature Prediction of a Gasoline Direct Injection Engine using Cylinder, Intake and Exhaust Pressures," *Control Eng. Pract.* 119 (2022): 104978, doi:10.1016/j.conengprac.2021.104978.
10. Galli, C., Ciampolini, M., Drovandi, L., Romani, L. et al., "Real-Time Control of Hydrogen Injection in a PFI Internal Combustion Engine based on an Online Physics-Based Model for Estimating Trapped Air and EGR," SAE Technical Paper 2024-32–0103, SAE International, Warrendale, PA, 2025, doi:10.4271/2024-32-0103.
11. Romani, L., Bosi, L., Ciampolini, M., Raspanti, S. et al., "Experimental Assessment of the Heat Losses Due to the Adoption of a Passive Prechamber in a Jet Ignition 4-Stroke Engine," SAE Technical Paper 2022-32–0060, SAE International, Warrendale, PA, 2022, doi:10.4271/2022-32-0060.
12. Raspanti, S., Ciampolini, M., Bigalli, S., Fabiani, A. et al., "Numerical Investigation on the Effects of the Setting of the Load Control System of a Formula SAE Single-Cylinder Turbocharged Engine on Fuel Efficiency and Performance," *J. Phys. Conf. Ser.* 2385, no. 1 (2022): 012081, doi:10.1088/1742-6596/2385/1/012081.
13. Galli, C., Superchi, F., and Bianchini, A., "Enhancing the Prediction of Electric Load Demand: A Comparative Analysis of ARIMA and ANN Models for the Case of a Small Touristic Island," *J. Phys. Conf. Ser.* 2893, no. 1 (2024): 012120, doi:10.1088/1742-6596/2893/1/012120.

Contact Information

Giovanni Ferrara
Department of Industrial Engineering,
Università degli Studi di Firenze,
Via di Santa Marta 3, 50139, Florence, Italy,
giovanni.ferrara@unifi.it

Abbreviations

AFR - Air-fuel ratio
BDC - Bottom dead center
BWD - Blowdown
CA - Crank angle
ECU - Engine control unit
EGR - Exhaust gas recirculation
EVC - Exhaust valve closing
EVO - Exhaust valve opening
GDI - Gasoline direction injection
ICE - Internal combustion engine
IMEP - Indicated mean effective pressure
IVC - Intake valve closing
k - Time-based index of the engine cycle
MAF - Mass air flow
MAP - Manifold absolute pressure
MIMO - Multi-input multi-output
NRMSPE - Normalized Root Mean Square Percentage Error
NMAPE - Normalized Mean Absolute Percentage Error
PFI - Port-fuel injection
SI - Spark ignition
TPA - Three-pressure- analysis

ISSN 0148-7191